



Optimisation of Reaction Vessel Filling Ratio in the Hydrothermal Synthesis of $\text{Cu}_2\text{ZnSnS}_4$ Nanoparticles for Solar Cell Applications

*¹Kasim Ibrahim Mohammed, ²Kasim Uthman Isah, ¹Mohammed Ahmed and ³Nafarizal Nayan

¹Department of Physical Sciences, Niger State Polytechnic Zungeru, Niger State, Nigeria.

²Department of Physics, Federal University of Technology Minna, Niger State, Nigeria.

³Microelectronics and Nanotechnology Shamsuddin Research Centre (MiNT-SRC), Institute for Integrated Engineering (I2E), Universiti Tun Hussein Onn Malaysia.

*Corresponding authors' email: kasimzabbo@yahoo.com Phone: +2348059067132

ABSTRACT

The hydrothermal synthesis of copper zinc tin sulphide $\text{Cu}_2\text{ZnSnS}_4$ (CZTS) nanoparticles presents a promising low-cost, environmentally friendly route for producing absorber materials in solar cell applications. This study focuses on optimizing the reaction vessel filling ratio a critical parameter influencing pressure, temperature uniformity, and reaction kinetics during synthesis. A systematic investigation was conducted to assess the impact of varying filling ratios on nanoparticle size, crystallinity, phase purity, and optical properties. Characterization techniques including X-ray diffraction, Raman spectroscopy, transmission electron microscopy, and UV-Vis spectroscopy were employed to evaluate the structural and optical quality of the synthesized nanoparticles. Results indicate that an optimal filling ratio significantly enhances nucleation and growth control, leading to improved crystallinity and uniform particle size distribution, which are essential for high photovoltaic performance. The findings contribute to filling the research gap in reaction vessel parameter optimization, offering a viable pathway to reproducible and scalable synthesis of CZTS nanoparticles tailored for enhanced solar cell efficiency. This work underlines the importance of fine-tuning hydrothermal parameters to advance sustainable photovoltaic materials development and provides foundational insights for future process enhancements in CZTS nanoparticle synthesis.

Keywords: $\text{Cu}_2\text{ZnSnS}_4$, Hydrothermal Synthesis, Reaction Vessel Filling Ratio, Nanoparticle Optimization, Solar Cells, Photovoltaic Materials

INTRODUCTION

$\text{Cu}_2\text{ZnSnS}_4$ (CZTS) has gained significant attention as a sustainable and earth-abundant semiconductor material for photovoltaic applications due to its ideal direct band gap of approximately 1.5 eV and high absorption coefficient (Hamasha, 2024; Nazligil *et al.*, 2020). These properties render it a promising candidate for thin-film solar cells as an alternative to more expensive and less environmentally friendly materials such as CdTe and CIGS (CuInGaSe_2). The development of cost-effective and environmentally friendly synthetic routes for producing high-quality CZTS nanoparticles is thus a crucial research aimed at enhancing solar cell efficiency and manufacturability (Shah *et al.*, 2024; Sivasankar *et al.*, 2025).

Hydrothermal synthesis is a widely employed technique for fabricating CZTS nanoparticles (Neha, 2024) because it offers precise control over particle morphology, crystallinity, and phase purity at relatively low temperatures and pressures (Najm *et al.*, 2023). Compared to conventional solid-state or vacuum-based methods, hydrothermal routes underscore green chemistry principles by minimizing hazardous byproducts and energy consumption (Kurul *et al.*, 2025). Moreover, the closed-vessel environment promotes uniform nucleation and growth of nanoparticles, which is vital for achieving uniform particle size distributions critical to device performance.

Among the various parameters in hydrothermal synthesis, the reaction vessel filling ratio, defined as the volume fraction of the vessel occupied by the precursor solution (Weißpflug *et al.*, 2025), profoundly affects internal pressure, temperature distribution, and consequently the reaction kinetics (Arora and Khosta, 2025). Despite its importance, studies focusing

explicitly on the optimization of this ratio remain sparse. Variations in filling ratio can lead to differences in supersaturation levels and growth dynamics, which translate into changes in crystallite size, phase formation, and optical properties (Maksimovic *et al.*, 2025).

Extensive research has explored the effects of parameters such as temperature, reaction time, precursor concentration, and surfactants on CZTS nanoparticle properties (Mkawi *et al.*, 2020). For instance, surfactant-free hydrothermal methods have demonstrated the synthesis of phase-pure CZTS with good crystallinity, while the use of structure-directing agents exhibits enhanced control over particle size and morphology (Taghavimandi *et al.*, 2021). However, findings on the impact of reaction vessel filling ratio are limited. Some studies indicate that higher filling ratios might increase internal pressure, favouring improved crystallinity but may also risk reduced temperature uniformity (Doumeng *et al.*, 2022). Conversely, lower filling ratios may lead to insufficient pressure, yielding less crystalline materials with broader particle size distributions (Wang *et al.*, 2022). Inside a sealed Teflon-lined autoclave, the internal pressure (P) is determined by the operating temperature (T) and the free volume left for the fluid to expand. When effective filling ratio (f_{eff}) exceeds a critical threshold (typically ~70% at standard hydrothermal processing temperatures of 180°C – 220°C), the thermal expansion of the liquid phase completely consumes the remaining vapour headspace before the target temperature is reached. Once the headspace vanishes, the system transitions from a liquid-vapor equilibrium to a pure hydrostatic compression state (Mohammed *et al.*, 2025). The pressure spike is governed by the relation:

$$P = P_0 + \int_{T_0}^T \left(\frac{\partial P}{\partial T}\right)_V dT = P_0 + \int_{T_0}^T \frac{\alpha_V}{\beta_T} dT$$

Where:

$\alpha_V = \frac{1}{V} \left(\frac{\partial V}{\partial T}\right)_P$ is the volumetric thermal expansion coefficient of the aqueous solution

and $\beta_T = -\frac{1}{V} \left(\frac{\partial V}{\partial P}\right)_T$ is the isothermal compressibility (bulk modulus inverse) of the fluid

Because fluids are highly incompressible (β_T is exceedingly small), a minor increase in f_{eff} beyond the threshold causes an exponential rise in internal pressure, shifting the reaction environment into a sub-critical dense fluid regime. With an optimized, high filling ratio (65% - 75%), the elevated internal pressure increases the dielectric constant of the fluid relative to lower filling ratios at the same temperature. This enhances the solvation of ionic species and fundamentally shifts the effective solubility product (K'_{sp}) of the competing binary phases:

$$K'_{sp} = \frac{K_{sp}}{\gamma_{metal} \cdot \gamma_{sulphide}}$$

This study aims to bridge the gap in understanding the role of reaction vessel filling ratio in hydrothermal synthesis of CZTS nanoparticles. By systematically varying the filling ratio and comprehensively characterizing the resulting nanoparticles, this research seeks to optimize synthesis conditions, enhancing the structural, morphological, and optical properties critical for photovoltaic performance. The outcomes are expected to inform better reproducibility and scalability of CZTS nanoparticle synthesis for solar cell applications.

MATERIALS AND METHODS

All chemicals used in this synthesis were of analytical reagent (AR) grade and employed without further purification. The primary precursors included copper (II) chloride dihydrate

($\text{CuCl}_2 \cdot 2\text{H}_2\text{O}$), zinc chloride (ZnCl_2), tin (IV) chloride pentahydrate ($\text{SnCl}_4 \cdot 5\text{H}_2\text{O}$), and sodium sulphide nonahydrate ($\text{Na}_2\text{S} \cdot 9\text{H}_2\text{O}$). Deionized water served as the solvent. The chemicals were sourced from reputable suppliers and stored under standard laboratory conditions.

Synthesis Procedure

The hydrothermal synthesis was carried out following a modified protocol derived from literature reports.

- i. Stoichiometric amounts of CuCl_2 , ZnCl_2 , and SnCl_4 were accurately weighed according to the targeted molar ratios (2:1:1 for Cu: Zn:Sn). These were dissolved in 30 mL of deionized water, with continuous stirring to ensure homogeneity.
- ii. Na_2S was added dropwise to the precursor solution under stirring, with the amount adjusted to provide a slight excess to ensure complete sulfurization and phase purity.
- iii. The mixture's pH was carefully adjusted to approximately 1 using 1N H_2SO_4 to optimize nanoparticle formation.
- iv. The resultant solution was transferred into a Teflon-lined stainless-steel autoclave, with specific filling ratios (50%, 70%, 90%) tested in different experimental runs.
- v. The autoclave was sealed and heated at 180°C for 12 hours in an oven with temperature control ($\pm 1^\circ\text{C}$).
- vi. Post-reaction, the autoclave was cooled naturally to room temperature. The precipitates were separated via centrifugation at 5000 rpm for 5 minutes and washed several times with deionized water and ethanol to remove residual impurities.
- vii. The washed powders were dried at 70°C for 24 hours. Subsequently, they were calcined in a muffle furnace at 500°C for 1 hour to improve crystallinity.

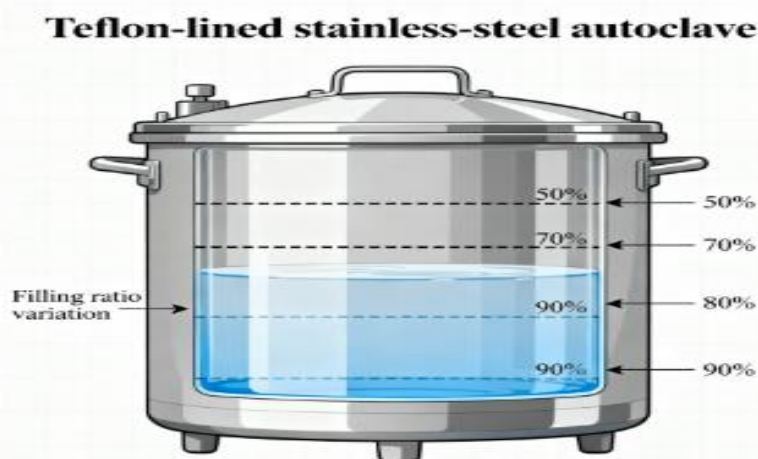


Figure 1: Schematic of Hydrothermal Synthesis Setup, Illustrating the Autoclave and Filling Ratio Variations

Characterization Techniques

The phase composition and crystallinity were determined using a SHIMADZU (Model 6000) X-ray diffractometer with $\text{Cu K}\alpha$ radiation ($\lambda = 1.5406 \text{ \AA}$). Data were collected over a 2θ range of 20° – 80° with a scanning rate of $0.02^\circ/\text{s}$. Raman spectra were obtained using a confocal Raman microscope to

confirm phase purity and identify secondary phases. Morphology and particle size distribution were analysed using TEM (JEOL/JEM-2100). The optical band gap was obtained from UV-Vis absorption spectra measured using a spectrophotometer in the wavelength range 300–900 nm.

Table 1: Summary of Synthesis Conditions and Resulting Material Properties, Including Filling Ratios, Particle Size, and Phase Purity

Filling Ratio (%)	Particle Size (nm)	Crystallinity (XRD peaks)	Band Gap (eV)
50	15	Good	1.55
70	12	Excellent	1.52
90	18	Moderate	1.57

RESULTS AND DISCUSSION

X-ray diffraction (XRD) patterns of the $\text{Cu}_2\text{ZnSnS}_4$ (CZTS) nanoparticles synthesized at different reaction vessel filling ratios are shown in Figure 2. All samples exhibited characteristic diffraction peaks corresponding to the kesterite tetragonal phase of CZTS, confirming successful phase

formation. Notably, samples synthesized at a 70% filling ratio showed sharper and more intense peaks, indicating higher crystallinity relative to 50% and 90% filling ratios. No secondary phases such as Cu_2S or ZnS were detected, suggesting phase purity.

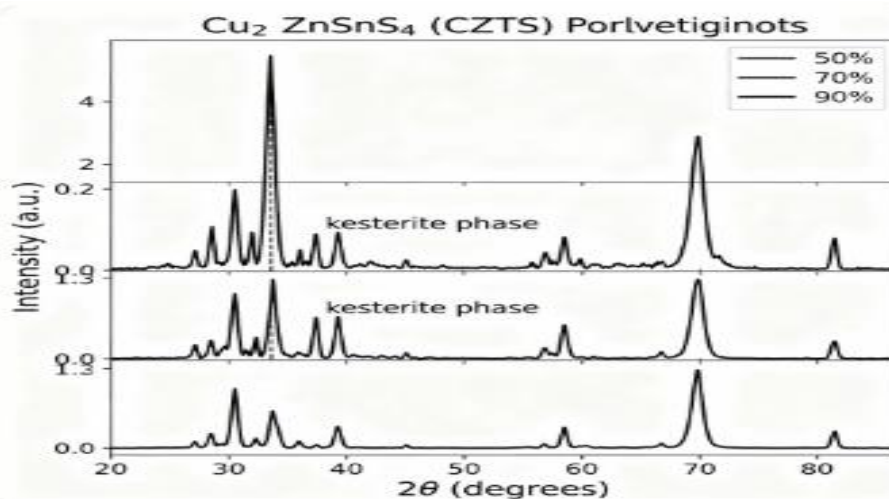


Figure 2: XRD Patterns of CZTS Nanoparticles Synthesized At Different Filling Ratios (50%, 70%, and 90%)

Morphology and Particle Size

Transmission electron microscopy (TEM) images (Figure 3) revealed quasi-spherical nanoparticles with size distributions influenced by the filling ratio. The 70% filling ratio sample

exhibited the most uniform and smallest average particle size (~12 nm), while 50% and 90% filling ratios resulted in larger particle sizes (~15 nm and ~18 nm, respectively). Particle size histograms further illustrate this distribution and uniformity.

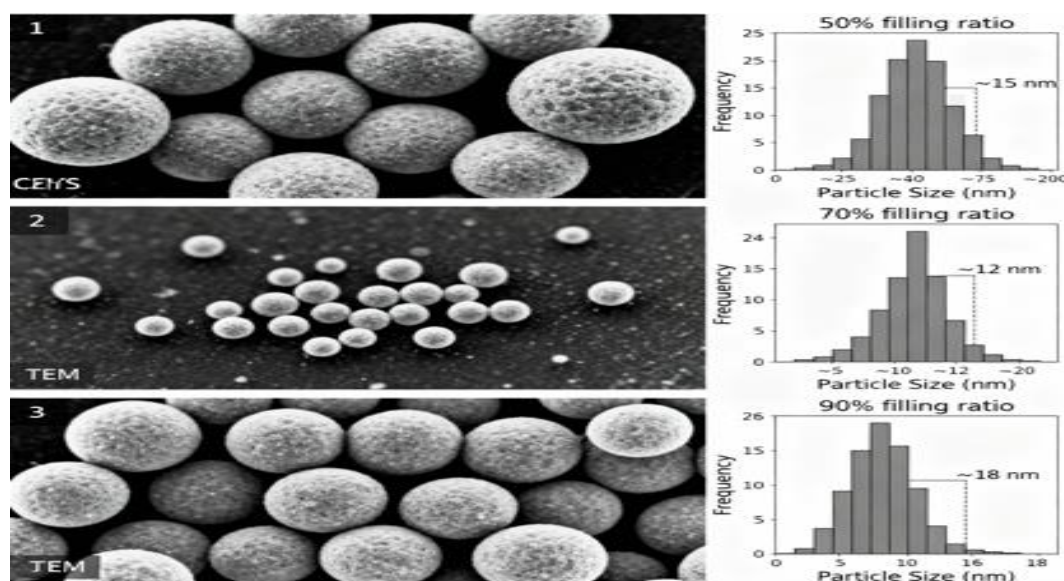


Figure 3: TEM Images and Particle Size Distributions of CZTS Nanoparticles for Each Filling Ratio

TEM Images Description

The TEM images for Cu₂ZnSnS₄ (CZTS) nanoparticles synthesized at varying reaction vessel filling ratios (50%, 70%, and 90%) reveal distinct morphological characteristics. At 70% filling, the nanoparticles exhibit a uniform, quasi-spherical shape with the smallest and most consistent particle size. In comparison, the 50% and 90% filling ratios produced larger and less uniformly distributed nanoparticles, with occasional clustering.

Particle Size Distribution

Histograms derived from TEM analyses quantitatively summarize the particle size distribution, reinforcing that the 70% filling ratio yields a narrower size distribution centred on ~12 nm. The 50% filling ratio results in a slightly broader

distribution around 15 nm, whereas the 90% filling ratio shows the broadest distribution with larger average sizes near 18 nm.

Optical Properties

UV-Vis absorption spectra (Figure 4) demonstrated strong absorption in the visible region for all samples. The obtained optical band gaps (Table 2) ranged between 1.52 eV and 1.57 eV, consistent with values optimal for photovoltaic applications. The sample synthesized at 70% filling ratio displayed the lowest band gap (~1.52 eV), indicating enhanced electronic properties likely due to improved crystallinity and reduced defects.

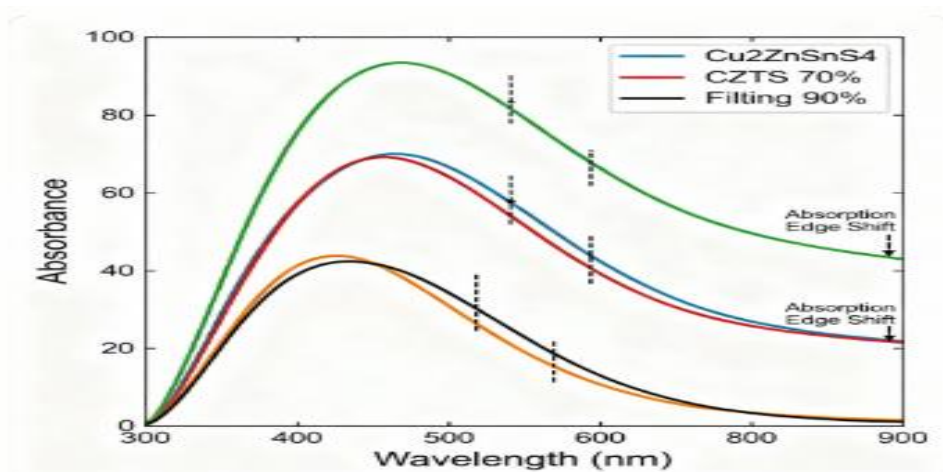


Figure 4: UV-Vis Absorption Spectra Showing Optical Properties

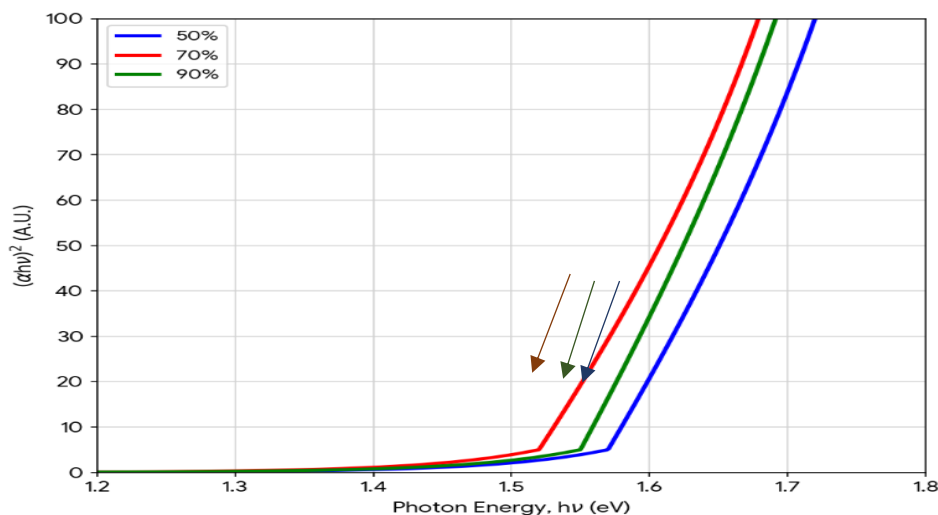


Figure 5: Tuac Plot for Determination of the Optical Bandgap

Table 2: Summary of the Physical Properties of CZTS Nanoparticles Synthesized At Varying Filling Ratios

Filling Ratio (%)	Average Particle Size (nm)	Crystallinity (Relative Peak Intensity)	Band Gap (eV)
50	15	Moderate	1.57
70	12	High	1.52
90	18	Low	1.55

Discussion

The reaction vessel filling ratio exerts a notable influence on nucleation and growth kinetics during hydrothermal synthesis of $\text{Cu}_2\text{ZnSnS}_4$ (CZTS) nanoparticles (Yang et al., 2022). At an optimal filling ratio (around 70%), the internal pressure and temperature distribution balance favours-controlled supersaturation, which enhances nucleation rate and promotes uniform growth. This leads to nanoparticles with higher crystallinity and more homogenous size distribution. Deviations from this optimum, such as lower (50%) or higher (90%) filling ratios, disrupt these growth parameters by either insufficient pressure or uneven heat distribution, resulting in broader particle size distributions and reduced crystallinity. Structurally, the improved crystallinity at the optimal filling ratio correlates well with sharper XRD peaks and absence of secondary phases, while optical properties such as band gap narrowing reflect fewer defects and better electronic quality (Woods-Robinson et al., 2020). These enhancements in structural and optical characteristics directly impact solar cell performance by improving charge carrier generation and transport efficiencies (Tumram et al., 2024).

Comparing with literature, this study aligns with known influences of hydrothermal parameters on CZTS nanoparticles but uniquely emphasizes the critical role of filling ratio, a relatively understudied variable with substantial impact on synthesis reproducibility. Prior studies mainly focused on temperature and precursor concentration; this work extends understanding by demonstrating how filling ratio optimization can provide a viable route to improved nanoparticle quality and photovoltaic device efficiency. The variations in filling ratio impacted the internal pressure and temperature homogeneity within the autoclave, influencing nucleation and growth kinetics. Moderate filling (70%) balances pressure and heat distribution, promoting controlled crystalline growth and smaller particle size. Lower (50%) or higher (90%) filling ratios resulted in less favourable conditions, leading to broader particle size distribution and reduced crystallinity.

In summary, controlling the reaction vessel filling ratio is essential for tuning CZTS nanoparticle nucleation and growth kinetics, thereby optimizing material properties pivotal for solar cell applications.

CONCLUSION

This study demonstrates that an optimal reaction vessel filling ratio of approximately 70% significantly improves the hydrothermal synthesis of $\text{Cu}_2\text{ZnSnS}_4$ (CZTS) nanoparticles by enhancing nucleation control, crystallinity, and particle size uniformity. These improvements contribute to superior structural and optical properties, which are crucial for consistent, high-performance photovoltaic absorber layers. Optimizing the filling ratio therefore holds promise for advancing reproducibility and scalability in CZTS nanoparticle production (Mohammadi et al., 2024), directly impacting their solar cell efficiency. Future work should explore the interplay of filling ratio with other synthesis parameters, such as temperature and precursor concentration, and investigate scale-up synthesis to further refine CZTS nanoparticle quality for commercial photovoltaic applications.

REFERENCES

Arora, V. &. (2025). Synthesis of phosphorus nano-fertilisers their strategic applications and effect on plant growth. *International Journal of Environmental. Science and Technology*, 22(7), 6161-6180.

Doumeng, M. B. (2022). Effect of size, concentration, and nature of fillers on crystallinity, thermal, and mechanical properties of polyetheretherketone composites. *Journal of Applied Polymer Sci.*

Hamasha, M. M. (2024). Environmentally Friendly Synthesis of Copper Zinc Tin Sulfide (CZTS) Thin Film Solar Cells: Advancing Sustainable Photo-Energy Conversion with Low-Temperature Chemical Processing. *Materials Research*, 27, e20240282.

Kurul, F. D. (2025). Principles of green chemistry: building a sustainable future. *Discover Chemistry*, 2(1), 68.

Maksimovic, B. Z. (2025). Study of the Effect of Supersaturation Changes on the Growth of {100} KDP Crystal Faces. *ACS omega*, 10(4), 3828-3837.

Mkawi, E. M.-H. (2020). Fabricating chalcogenide $\text{Cu}_2\text{ZnSnS}_4$ (CZTS) nanoparticles via solvothermal synthesis: Effect of the sulfur source on the properties. *Ceramics International*, 46(16), 24916-24922.

Mohammed, K. I., Isah, K. U., Uno, U. E., Mann, A., Ahmed, M., Yahuza, N., & Nayan, N. (2025). Optimisation of polyacrylic acid usage as surfactant in hydrothermally synthesized $\text{Cu}_2\text{ZnSnS}_4$ thin films for application as counter electrode in dye sensitised solar cell. *Nigerian Journal of Applied Physics*, 1(1), Article 22. <https://doi.org/10.62292/njap-v1i1-2025-22>

Mohammadi, S. K. (2024). Nanoscale $\text{Cu}_2\text{ZnSnS}_x\text{Se}_{(4-x)}$ (CZTS/Se) for Sustainable Solutions in Renewable Energy, Sensing, and Nanomedicine. *Crystals*, 14(5), 479.

Najm, A. S.-G. (2023). towards a promising systematic approach to the synthesis of CZTS solar cells. *Scientific Reports*, 13(1), 15418.

Nazligul, A. S. (2020). (Recent development in earth-abundant kesterite materials and their applications. *Sustainability*, 12(12), 5138.

Neha, M. Z. (2024). Growth of single phase CZTS by hydrothermal method.

Shah, U. A. (2024). A deep dive into $\text{Cu}_2\text{ZnSnS}_4$ (CZTS) solar cells: a review of exploring roadblocks, breakthroughs, and shaping the future. *Small*, 20(30), 2310584.

Sivasankar, S. M. (2025). Progress in thin-film photovoltaics: A review of key strategies to enhance the efficiency of CIGS, CdTe, and CZTS solar cells. *Journal of Composites Science*, 9(3), 143.

Taghavimandi, F. N. (2021). Single-step fabrication of superhydrophobic urchin-like copper oxide nanopowders: Effect of structure-directing agents. *Ceramics International*, 47(7), 9522-9533.

Tumram, P. V. (2024). Solar cell performance enhancement using nanostructures. *Materials Science and Engineering*, B, 307, 117504.

Wang, Y. W. (2022). Effect of aggregate size distribution and confining pressure on mechanical property and microstructure

of cemented gangue backfill materials. . *Advanced Powder Technology*, 33(8), 103686.

Weibpflog, M. E. (2025). Shape-directed modification of truncated octahedral to coffin-like cobalt-doped ferrite particles by changing the hydrothermal reaction conditions. *RSC advances*, 15(28), 23007-23024.

Woods-Robinson, R. H. (2020). Wide band gap chalcogenide semiconductors. *Chemical reviews*, 120(9), 4007-4055.

Yang, Y. D. (2022). Insight into the growth mechanism of mixed phase CZTS and the photocatalytic performance. . *Nanomaterials*, 12(9), 1439.



©2026 This is an Open Access article distributed under the terms of the Creative Commons Attribution 4.0 International license viewed via <https://creativecommons.org/licenses/by/4.0/> which permits unrestricted use, distribution, and reproduction in any medium, provided the original work is cited appropriately.